

Nonlinear Dynamics of a Bose-Einstein Condensate in a Magnetic Waveguide

H. Ott,* J. Fortágh, S. Kraft, A. Günther, D. Komma, and C. Zimmermann

*Physikalisches Institut der Universität Tübingen
Auf der Morgenstelle 14, 72076 Tübingen, Germany*

(Dated: May 21, 2019)

We have studied the internal and external dynamics of a Bose-Einstein condensate in an anharmonic magnetic waveguide. An oscillating condensate experiences a strong coupling between the center of mass motion and the internal collective modes. Due to the anharmonicity of the magnetic potential, not only the center of mass motion shows harmonic frequency generation, but also the internal dynamics exhibit nonlinear frequency mixing. We describe the data with a theoretical model to high accuracy. For strong excitations we test the experimental data for indications of a chaotic behavior.

PACS numbers: 03.75.Kk, 03.75.Be, 05.45.-a

Since the first realization of Bose-Einstein condensates in 1995 ideas have been discussed how to exploit this new form of matter for atom optics. Atom interferometry with single atoms has been extensively investigated in the past decade [1] and finds important applications for high precision measurements of gravitational or rotational forces [2, 3]. It was also possible to realize and demonstrate a number of atom optical elements such as mirrors [4], gratings [5], beamsplitters [6] and waveguides [7, 8]. It is a fascinating vision to integrate these elements on a microfabricated atom chip, where lithographically produced wires generate spatially and temporally variable potentials for atoms with almost any desired complexity. Extremely sensitive chip based sensors for forces and accelerations as well as for applications in quantum computing are conceivable. Since Bose-Einstein condensates have been loaded into microfabricated traps [9, 10] this vision has changed into a very real research topic. One of the most urgent questions to ask about is the suitability of condensates for integrated atom optics.

In conventional atom optics experiments with thermal atoms, the interaction between the atoms plays no significant role. For Bose-Einstein condensates this is substantially different and the wave function must be described by the Gross Pitaevskii equation which gives raise to novel nonlinear effects. For condensates in a harmonic trapping potential, the center of mass (CM) motion is completely decoupled from the internal dynamics [11] and the condensate dynamic is given by a simple sinusoidal CM oscillation. However, the trapping potentials of atom chips are typically anharmonic. In this letter we will show that in this case the CM motion induces a significant excitation of the collective modes of the condensate. Nonlinear coupling between the collective modes occurs and even a chaotic behavior is possible.

We present a detailed experimental study of the condensate dynamics in the most fundamental atom optical element — a magnetic waveguide. The linear propagation of Bose-Einstein condensates along a non terminated guide was recently investigated in Refs. [13] and [14].

Here we regard waveguides which are closed at both ends such that the generic motion of the condensate is now a periodic oscillation. In our experiment the oscillation is started by displacing the condensate from the potential minimum of the waveguide by up to 1 mm and then release it into the axially anharmonic trapping potential of the guide. We have measured the time evolution of the CM motion and of the aspect ratio i.e. the ratio between the radial and the axial condensate radii. With increasing initial displacement, the fundamental frequency of the CM motion ν_0 changes and higher harmonics of ν_0 appear in the frequency spectrum. During the oscillation, the condensate travels along a waveguide, whose potential curvature is spatially changing. In its rest frame, the condensates thus experiences a time-dependent change of the trapping potential which leads to a shape oscillation at the driving frequency ν_0 and its first harmonic. In addition, the lowest lying collective mode of the condensate is off-resonantly excited. For strong excitations, sums and differences of these three frequencies appear due to the nonlinearity of the internal dynamics of the condensate. To describe the experimental data we have developed a theoretical model which is described in Ref. [15]. The model is based on the separation of the CM motion and reduces the internal dynamics to that of a condensate in a fictitious time-dependent harmonic potential. Such a scenario is known to be exactly solvable in Thomas-Fermi approximation [16, 17]. The model also allows us to identify an experimentally accessible regime where the dynamics become chaotic.

In our experiment we prepare a ^{87}Rb condensate in the ($F = 2, m_F = 2$) ground state in a magnetic microtrap. The apparatus including the microstructure for generating the microtrap is described in detail elsewhere [9, 18]. The trapping frequencies are 8 Hz in the axial and 110 Hz in the radial direction. The initial cloud contains about 100,000 atoms with a central density of $5 \times 10^{13} \text{ cm}^{-3}$. This ensures a condensate lifetime of 1 s. To induce the oscillation we displace the condensate within 400 ms with a magnetic field gradient and switch off the field gradi-

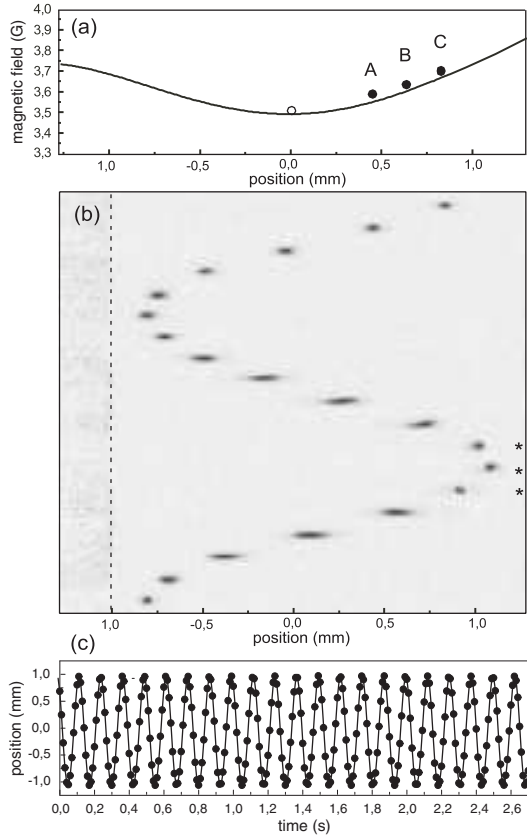


FIG. 1: Oscillation of the condensate in an anharmonic trapping potential. (a) Magnetic field in the trap minimum along the axial direction. The black dots indicate the starting positions of the oscillation for each experimental series (see Tab. I). The circle marks the initial position without displacement. (b) Absorption images (10 ms intervals) of the condensate after 20 ms time of flight (series C, 10 ms intervals). Due to the time of flight, the amplitude of the oscillation is enhanced with respect to oscillation in the trap (also a phase shift occurs). For condensates marked with an asterisk the absorption images show diffraction and the aspect ratio can not be determined properly. (c) CM motion of the condensate (series B): experimental data (dots) and fit with three sinusoidal functions (line).

ent non-adiabatically ($< 60 \mu\text{s}$). The waveguide potential is characterized by an almost constant radial oscillation frequency (the maximal deviations are smaller than 10 percent) and a strongly varying axial curvature. The axial potential $U(x)$ was numerically determined to

$$\frac{U(x)}{\mu} [\text{G}] = 0.219x^2 - 0.013x^3 - 0.033x^4 - 0.007x^5, \quad (1)$$

where x has to be quoted in millimeter and μ is the magnetic moment of the atom. The shape of the axial potential is sketched in Fig. 1a. The experiment was performed for three different initial displacements d : 0.45 mm (A), 0.63 mm (B) and 0.79 mm (C). Tab. I summarizes the parameters of the three data series. In Fig. 1b the first 1.5

Data series	d	ν_{sp}	T	N_{data}
A	0.45 mm	200 Hz	1.015 s	204
B	0.63 mm	100 Hz	2.700 s	271
C	0.79 mm	200 Hz	0.765 s	154

TABLE I: Parameters for the three data series: initial displacement d , sampling rate ν_{sp} , observed oscillation period T and number of data points N_{data} .

oscillation periods of series C are shown. To determine the CM position and the aspect ratio, the absorption images are fitted with a Thomas-Fermi profile. The aspect ratio bears the advantage of being independent from the atom number. To exclude influences of the nearby copper conductors [19, 20], the experiment was carried out in a distance to the surface of $220 \mu\text{m}$.

The CM motion is almost undamped and shows a very high quality factor (Fig. 1c). For series B with a length of 2.7 s we find a value of 20,000 which corresponds to a $(1/e)$ -lifetime of the oscillation of at least 40 minutes. Due to the anharmonicity of the potential (1), the frequency spectrum of the CM motion shows second and third harmonic generation. For series C with the largest initial displacement, the nonlinear effects are most pronounced and lead to a relative amplitude of 5 percent for the second harmonic and 1 percent for the third harmonic frequency with respect to the amplitude for the fundamental frequency ν_0 . For small amplitudes ν_0 amounts to 8.5 Hz but is reduced with increasing displacement (A, B, and C) by 4, 6, and 11 percent respectively. Because of the extremely low damping, the CM motion is suited to detect small forces, which may shift the trapping potential. An estimate for our experimental parameters indicates a resulting sensitivity of $F/m = 10^{-4}g$, with the gravitational acceleration g .

Concerning the internal dynamics the aspect ratio of the condensate and the theoretical model [15] are shown in Fig. 2. The model describes the condensate in an external potential $U(\mathbf{x})$ with a set of two coupled equation systems: the equation of motion for the center of mass

$$m\ddot{\mathbf{R}} = -\nabla U(\mathbf{R}), \quad (2)$$

and the coupled equations of motion for the three scaling factors [16, 17] for the Thomas-Fermi radii $r_i(t) = \lambda_i(t)r_i(0)$

$$\ddot{\lambda}_i = \frac{\omega_{i0}^2}{\lambda_i \lambda_1 \lambda_2 \lambda_3} - \frac{1}{m} \frac{\partial^2}{\partial^2 x_i} U(\mathbf{R}) \lambda_i, \quad i = 1, 2, 3, \quad (3)$$

where the second term on the right hand side establishes the coupling between the CM motion and the internal dynamics. The initial conditions for $t = 0$ are $\lambda_i(0) = 1$, $\dot{\lambda}_i(0) = 0$, $R(0) = d$ and $\dot{R}(0) = 0$. The oscillation frequency of the potential at $t = 0$ is given by ω_{i0} . While

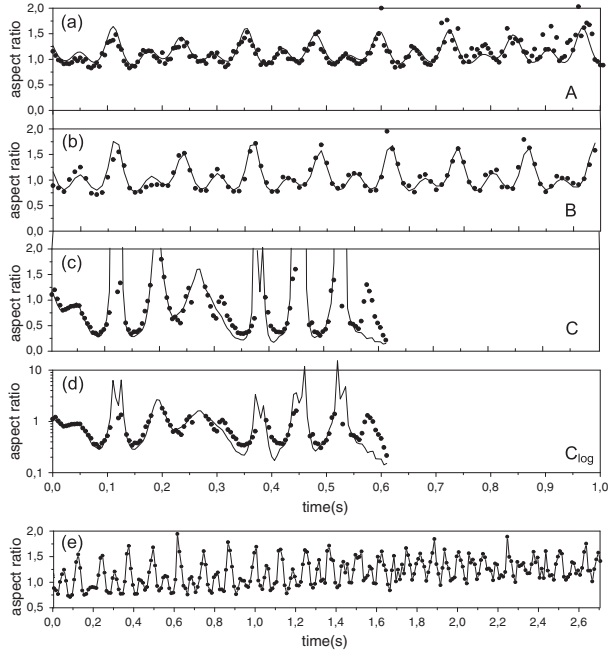


FIG. 2: Evolution of the aspect ratio of the condensate for the data series A (a), B (b), and C (c) (dots) and theoretical model (solid line). (d) Plot (c) with a logarithmic scale. (e) All data points of series B.

the theory contains no free parameter, a constant multiplication factor of 1.2 was needed to describe the data accurately. This may arise from a systematic error in the imaging system and analysis. Aside from this factor, the agreement is remarkable and proves true the picture that the external motion in an anharmonic potential leads to a time-dependent harmonic potential in the rest frame. In Fig. 1b, the condensates marked with an asterisk cannot be spatially resolved by our absorption imaging system, indicating an axial extension of the condensate of less than $15\ \mu\text{m}$. Therefore, the condensate may in fact follow the strong dynamics, which is predicted by the theory (Fig 2d). For the present data, we measure a change in the aspect ratio by more than a factor of 10, the largest value reported so far. The data of series B which cover 2.7s are promising to find effects arising from loss of atoms. At the end of the series, the atom number has dropped by more than a factor of 15 with only 3000 atoms left in the condensate. The evolution of the aspect ratio is shown in Fig. 2e. The systematic increase of the aspect ratio is due to the crossover to the 1D regime as defined in Ref. [21]. The Thomas-Fermi approximation breaks down because the chemical potential of the condensate becomes smaller than the radial kinetic energy, which then dominates the radial expansion of the condensate.

We have performed a frequency analysis of the aspect ratio with an algorithm suitable for unequally spaced or missing data [22]. The results are shown in Fig. 3. The

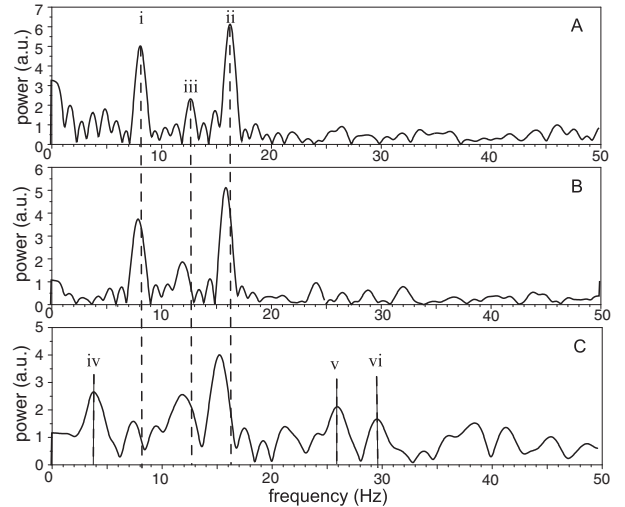


FIG. 3: Frequency spectra of the aspect ratio. The frequencies of the labeled peaks are: (i) fundamental frequency ν_0 , (ii) second harmonic frequency $2\nu_0$, (iii) quadrupole resonance frequency $\nu_q \simeq \sqrt{5/2}\nu_0$, (iv) difference frequency $2\nu_0 - \nu_q$, (v) sum frequency $2\nu_0 + \nu_q$ and (vi) fourth harmonic frequency $4\nu_0$.

spectra show three major frequencies: the fundamental frequency ν_0 (peak (i) in Fig. 3), the second harmonic (ii) and the resonance frequency ν_q of the lowest lying collective mode (iii). The latter does not deviate more than 4 percent from its small amplitude value for strongly anisotropic traps which is given by $\sqrt{5/2}\nu_0$. Furthermore, the spectrum for series C (Fig. 3) shows several mixed frequencies. Two of them, the sum and the difference between the second harmonic frequency and the lowest resonance frequency $2\nu_0 - \nu_q$ and $2\nu_0 + \nu_q$ have been identified ((iv) and (v)). This gives evidence for the nonlinear coupling of the collective excitations. Other than the coupled modes observed by Hechenblaikner *et al.* [23], the mode coupling in our experiment is non-resonant, and the mixed frequencies vanish in the limit of small amplitudes. Because the condensate performs a free oscillation in an external potential the total energy of the system is conserved. Summing up only the contributions for the internal energy of the condensate, one finds that the sum is not constant. Adding the kinetic and potential energy of the CM motion, the energy is conserved, which can be verified by using a Hamiltonian formalism [15]. Therefore, not only the internal dynamics is affected by the external motion, but there is also an energy exchange between the internal dynamics and the CM motion. In our experiment this effect leads to a theoretically calculated amplitude variation for the CM motion of $1/4000$, which is too small to be detected.

Fig. 4a shows absorption images for an initial displacement of 0.94 mm . The data show a strong axial excitation of the condensate, which raises the question of the onset of chaos. A signature of a chaotic behavior in experimen-

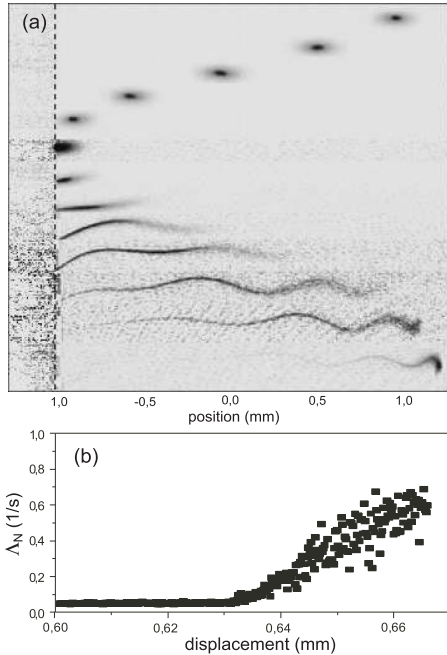


FIG. 4: (a) Oscillation for an initial displacement of 0.94 mm. The absorption images are taken after 20 ms time of flight. The vertical dotted line indicates the surface of a wire which narrows the display window. (b) Lyapunov exponent: $\Lambda_N = 1/(N\tau) \sum_{i=1}^N \ln d_i/d_0$ as a function of the initial displacement d . d_0 is the initial Euclidian distance between two neighboring trajectories, τ is the duration of one iteration and N is the number of iterations. The Lyapunov exponent is defined in the limit $\Lambda = \lim_{N \rightarrow \infty} \Lambda_N$. Each pair of trajectories was numerically solved for 200 s ($d_0 = 0.1 \mu\text{m}$, $\tau = 1 \text{ ms}$, $N = 2 \times 10^5$). Above a displacement of 0.67 mm the numerics are no longer stable for the total propagation time.

tal data is an enhanced noise in the frequency spectrum of the data. The spectrum of the aspect ratio for series C in Fig. 3 clearly shows an enhanced background, compared to the two other series. However, this should not be regarded as an unchallengeable experimental proof. Such a proof would require a longer data set and an enhanced resolution of the imaging system. Nevertheless, the theoretical model can be analyzed for the experimental parameters. One of the strongest evidences for a chaotic dynamic is a positive Lyapunov exponent, which indicates an exponential sensitivity to the initial conditions. For this purpose neighbouring trajectories for slightly different initial displacements have been simulated over 200 s. Fig. 4 shows the evolution of the Lyapunov exponent with increasing displacement. For a displacement of more than 0.63 mm, the calculated Lyapunov exponent becomes positive and grows linearly. As the total energy of the system is conserved, one can easily test the numerical stability and exclude any numerical artefacts. The corresponding Poincaré maps and the frequency spectra

of the trajectories indicate the same results. This gives strong evidence, that series C was performed in a regime where the longtime behavior of the trajectory is chaotic.

In conclusion, we have studied the dynamics of a Bose-Einstein condensate oscillating in an anharmonic trapping potential. We have identified several nonlinear effects including second and third harmonic generation of the center of mass motion, a coupling of the internal and external dynamics and nonlinear mode mixing. The theoretical model describes these effects with high accuracy. The model predicts a chaotic dynamic above a critical oscillation amplitude and the experimental data give indication for a chaotic motion too. In future experiments it will be important to characterize the chaotic regime. Thereby, loss of atoms and instability of the condensate may become important. Considering applications of magnetic microtraps and integrated atom optics, we have shown that a motion of a condensate in a magnetic waveguide necessarily leads to excitations of the inner degrees of freedom. For quantitative measurements, especially for interferometric arrangements, the nonlinear dynamics have to be taken into account.

We gratefully acknowledge financial support from the Deutsche Forschungsgemeinschaft under Grant No. Zi/419-5.

* Electronic address: ott@pit.physik.uni-tuebingen.de

- [1] *Atom Interferometry*, edited by Paul Berman (Academic Press, Chestnut Hill, MA, 1997).
- [2] F. Riehle *et al.*, Phys. Rev. Lett. **67**, 177 (1991).
- [3] M. Kasevich and S. Chu, Phys. Rev. Lett. **67**, 181 (1991).
- [4] K. S. Johnson *et al.*, Phys. Rev. Lett. **81**, 1137 (1998).
- [5] E. M. Rasel *et al.*, Phys. Rev. Lett. **75**, 2633 (1995).
- [6] D. Cassettari *et al.*, Phys. Rev. Lett. **85**, 5483 (2000).
- [7] M. Key *et al.*, Phys. Rev. Lett. **84**, 1371 (2000).
- [8] D. Müller *et al.*, Phys. Rev. Lett. **83**, 5194 (1999).
- [9] H. Ott *et al.*, Phys. Rev. Lett. **87**, 230401 (2001).
- [10] W. Hänsel *et al.*, Nature **413**, 498 (2001).
- [11] J. F. Dobson, Phys. Rev. Lett. **73**, 2244 (1994).
- [12] L. Deng *et al.*, Nature **398**, 218 (1999).
- [13] A. E. Leanhardt *et al.*, Phys. Rev. Lett. **89**, 040401 (2002)
- [14] J. Fortágh *et al.*, to be published in Appl. Phys. B
- [15] H. Ott *et al.*, cond-mat/0212193
- [16] Y. Kagan, E. L. Surkov, and G. V. Shlyapnikov, Phys. Rev. A **55**, R18 (1997).
- [17] Y. Castin and R. Dum, Phys. Rev. Lett. **77**, 5315 (1996).
- [18] J. Fortágh *et al.*, Appl. Phys. Lett. **81**, 1146 (2002).
- [19] J. Fortágh *et al.*, Phys. Rev. A **66**, 041604(R) (2002)
- [20] S. Kraft *et al.*, J. Phys. B: At. Mol. Opt. Phys. **35**, L469 (2002).
- [21] A. Görlitz *et al.*, Phys. Rev. Lett. **87**, 130402 (2001)
- [22] N. R. Lomb, Astrophys. Space Sci. **39**, 447 (1976).
- [23] G. Hechenblaikner *et al.*, Phys. Rev. Lett. **85**, 692 (2000).